Published in final edited form as:
Cancer Res. 2009 January 1; 69(1): 329–337. doi:10.1158/0008-5472.CAN-08-0613.

Interleukin-6 in the bone marrow microenvironment promotes the growth and survival of neuroblastoma cells

Tasnim Ara[1], **Liping Song**[1], **Hiroyuki Shimada**[2], **Nino Keshelava**[1], **Heidi V. Russell**[5], **Leonid S. Metelitsa**[1], **Susan G. Groshen**[3], **Robert C. Seeger**[1], and **Yves A. DeClerck**[1,4]

[1]Division of Hematology-Oncology, Department of Pediatrics, Keck School of Medicine of the University of Southern California and The Saban Research Institute of Childrens Hospital Los Angeles, Los Angeles, California

[2]Department of Pathology, Keck School of Medicine of the University of Southern California and The Saban Research Institute of Childrens Hospital Los Angeles, Los Angeles, California

[3]Department of Preventive Medicine, Keck School of Medicine of the University of Southern California and The Saban Research Institute of Childrens Hospital Los Angeles, Los Angeles, California

[4]Department of Biochemistry and Molecular Biology, Keck School of Medicine of the University of Southern California and The Saban Research Institute of Childrens Hospital Los Angeles, Los Angeles, California

[5]Department of Pediatrics, Baylor College of Medicine, Houston, Texas

Abstract

Neuroblastoma, the second most common solid tumor in children, frequently metastasizes to the bone marrow and the bone. Neuroblastoma cells present in the bone marrow stimulate the expression of interleukin-6 (IL-6) by bone marrow stromal cells (BMSC) to activate osteoclasts. Here we have examined whether stromal-derived IL-6 also has a paracrine effect on neuroblastoma cells. An analysis of the expression of IL-6 and its receptor IL-6R in 11 neuroblastoma cell lines indicated the expression of IL-6 in 7 cell lines and of IL-6R in 9 cell lines. Treatment of IL-6R positive cells with rhIL-6 resulted in STAT-3 and Erk 1/2 activation. Culturing IL-6R positive neuroblastoma cells in the presence of BMSC or rhIL-6 increased proliferation and protected tumor cells from etoposide-induced apoptosis, whereas it had no effect on IL-6R negative tumor cells. *In vivo*, neuroblastoma tumors grew faster in the presence of a paracrine source of IL-6. IL-6 induced the expression of cyclooxygenase-2 in neuroblastoma cells with concomitant release of prostaglandin-E2, that increased the expression of IL-6 by BMSC. Supporting a role for stromal-derived IL-6 in patients with neuroblastoma bone metastasis, we observed elevated levels of IL-6 in the serum and bone marrow of 16 patients with neuroblastoma bone metastasis, and in BMSC derived from these patients. Altogether the data indicate that stromal-derived IL-6 contributes to the formation of a bone marrow microenvironment favorable to the progression of metastatic neuroblastoma.

Keywords

neuroblastoma; interleukin-6; STAT-3; cell proliferation; apoptosis; tumor microenvironment

Requests for reprints: Yves A. DeClerck, MD Division of Hematology-Oncology, MS#54 Childrens Hospital Los Angeles 4650 Sunset Boulevard Los Angeles, CA 90027 declerck@usc.edu Tel: 323-361-2150 Fax: 323-664-9455.

Introduction

It has become increasingly apparent that factors that influence the progression of cancer cells not only originate from genetic and epigenetic alterations in malignant cells but also from interactions between tumor cells and non-malignant cells in the tumor microenvironment (1-3). The tumor microenvironment does not only influence the growth of primary tumors but also plays a critical role in the development of distant metastasis, a role initially recognized more than 100 years ago by Paget (4). The bone marrow and the bone, which are among the most common sites of metastasis in cancer, provide a soil that is particularly favorable to the progression of cancer cells. They are a reservoir of numerous stimulatory cytokines and growth factors, and provide a sanctuary against the cytotoxic effects of chemotherapy (5,6). The bone marrow contains two distinct populations of stem cells that contribute to cancer progression. The first consists of hematopoietic stem cells located in the endosteal niche. When mobilized toward the vascular niche these cells mature into vascular endothelial growth factor receptor (VEGFR)-1 and -2 expressing cells, that are recruited by the primary tumor where they contribute to inflammation and vascularization. VEGFR-1 positive cells also colonize distant organs where they form pre-metastatic niches (7). The second population is made of mesenchymal stem cells. These cells give rise to a broad spectrum of stromal cells, including osteoblasts, osteocytes, chrondrocytes, smooth muscle cells, adipocytes, fibroblasts, myofibroblasts, and cardiac muscle cells, and have the capacity to repair injured tissues (8,9). These cells express a variety of cell surface-associated markers like STRO-1, CD105, CD44 and CD166 (10,11). Their role in cancer progression is still poorly understood.

Neuroblastomas are biologically heterogeneous tumors of neural crest origin and represent the second most common solid tumor in children (12). Despite major progress in our understanding of the biology of this type of cancer and in the treatment of these patients with intensive myeloablative chemotherapy, bone marrow transplantation and retinoic acid therapy (13), metastasis remains the leading cause of morbidity and mortality. It is present in approximately 60% of children with neuroblastoma at the time of diagnosis, with the most common sites of metastasis being the bone marrow, the bone and the liver (14). Bone metastasis in neuroblastoma is characterized by the presence of osteolytic lesions caused by an increase in osteoclast activation (15). We have previously reported that most neuroblastoma cells do not produce osteoclast activating factors like parathyroid hormone-related peptide (PTHrP) or receptor activator of NFκB ligand (RANKL) typically produced by metastatic breast cancer cells, but stimulate the production of interleukin-6 (IL-6) by bone marrow stromal cells (BMSC) which is a potent activator of osteoclasts (16).

Interleukin-6 (IL-6) is a pleiotropic cytokine that exerts its effect through interaction with the IL-6 receptor complex composed of an α-chain subunit (IL-6Rα/gp80) and a β-chain subunit (gp130) (17,18). Whereas many cells express gp130, the expression of the IL-6Rα/gp80 provides the specificity of the response to IL-6 (17). Binding of IL-6 to its heterodimeric receptor leads to conformational changes in the gp130 subunit, that through activation of Janus kinases (Jak), activates members of the signal transducer and activator of transcription (STAT) family of proteins and the extracellular signal regulated kinases (Erk1/2) pathway (19-21). IL-6Rα/gp80 can be present in a soluble form (sIL-6R) generated by either alternate splicing or proteolytic shedding of the membrane-associated receptor. It acts as an agonist and potentiates the activity of IL-6 (22). Cells lacking IL-6Rα/gp80 can therefore become sensitive to IL-6 in the presence of sIL-6R (23).

The observation that neuroblastoma cells increase the expression of IL-6 by BMSC raised the question whether IL-6, in addition to activating osteoclasts, could also have a paracrine effect on tumor cells within the bone marrow microenvironment. Supporting this concept,

we demonstrate in this paper that neuroblastoma cells respond to IL-6 and that IL-6 stimulation provides them with a proliferative and a survival advantage.

Material and Methods

Cell cultures

Eleven cell lines with and without MYCN amplification were obtained from Dr. C. Patrick Reynolds (Childrens Hospital Los Angeles, Los Angeles, CA) with the exception of NB-19 cells, which were obtained from RIKEN (BioResource Center, Tsukuba, Japan). SAOS-2 and MG-63 human osteosarcoma cells were purchased from American Type Culture Collection. CHLA-255/Luc expressing the firefly luciferase reporter gene were used as previously reported (24). CHLA-255 cells overexpressing hIL-6 were obtained by incubating cells with the viral supernatant of 293 FT cells expressing a lentivirus (pLenti4/TO/V5-DEST vector; Invitrogen) in which hIL-6 cDNA was inserted using LR clonase. IL-6 expressing cells were selected in the presence of zeocin. These cells produced an average of 2.6 ng hIL-6/ml over 24h. Human BMSC were either purchased from ALLCells LLC (Emeryville, CA) or obtained from bone marrow samples of patients with neuroblastoma enrolled by the Children's Oncology Group. These samples were infiltrated with neuroblastoma cells (20% in sample NB-208 and 80% in sample NB-209). Mononuclear cells were separated by density gradient centrifugation over Ficoll-Hypaque using a human mesenchymal stem cell enrichment cocktail according to a previously reported procedure (25).

Reagents

Recombinant human IL-6 (rhIL-6), rhsIL-6R, mouse monoclonal antibodies (mAb) against IL-6Rα/gp80 and gp130 were purchased from R&D Systems (Minneapolis, MN). Rabbit polyclonal antibodies against phospho-STAT-3, STAT-3, phospho-Erk 1/2, and Erk 1/2 were purchased from Cell Signaling Technology, Inc. (Beverly, MA). Mouse mAb against β-tubulin and non-specific mouse IgG were obtained from Sigma Aldrich (St. Louis, MO). An unconjugated anti-human STRO-1 mouse mAb was purchased from R&D Systems. PEconjugated anti-human CD166, FITC-conjugated anti-human CD44, unconjugated anti-human CD34 and unconjugated anti-CD105 mouse mAb were purchased from BD Pharmingen (San Jose, CA). PE-conjugated mouse monoclonal antibodies against IL-6Rα/gp80 and gp130 and PE-conjugated mouse IgG were purchased from BD Biosciences (San Jose, CA), and used for FACS analysis. The MEK1 kinase inhibitor PD98059 and the Jak/STAT-3 inhibitor AG490 were purchased from Calbiochem (La Jolla, CA) and stored as 50 mM stock solution in dimethylsulfoxide at −20°C.

Reverse-Transcriptase Polymerase Chain Reaction (RT-PCR)

Two μg of RNA were reverse-transcribed with 200 U of Superscript III reverse-transcriptase (First-strand cDNA superscript III kit, Invitrogen, Carlsbad, CA) into cDNA in the presence of 0.5 nmol of oligo (dt) primer. RT-PCR were performed in 50 μl of reaction volume containing 2 μl of cDNA, 500 nmol of the corresponding primer sets and 2 U of Taq polymerase (Invitrogen). The following primer sets were used: IL-6 forward: 5'-TAGCCGCCCCACACAGACAG-3′ and reverse: 5′-GGCTGGCATTTGTGGTTGGG-3′; IL-6Rα/gp80 forward: 5′-CATTGCCATTGTTCTGAGGTTC-3′ and reverse: 5′-GTGCCACCCAGCCAGCTATC-3′; gp130 forward: 5′-GCAAGATGTTGACGTTGCAGAGACTTG-3, and reverse: 5′-GGGCATTCTCTGCTTCTACCCAGAC-3′; sIL-6R forward: 5′-CAGCAGTTCAAGAAGACGTGGAAGCT-3′ and reverse: 5′-GTGCCACCCAGCCAGCTATC-3′ these primers recognize the alternate spliced mRNA of

IL-6R/gp80; human GAPDH forward: 5′-ACAGTCAGCCGCATCTTCTT-3′, and reverse 5′-TTCTAGACGGCAGGTCAGGT-3′.

IL-6 and sIL-6R levels

Levels of human IL-6 and sIL-6R in the medium of cultured cells and in the serum and supernatant of bone marrow samples of patients with neuroblastoma were determined in triplicate aliquots by Enzyme Linked Immunoabsorbance Assay (ELISA) according to the manufacturer's protocol (Quantikine Immunoassay kit from R&D).

Western blot

Equal amounts of protein (20 μg) were loaded in each well and electrophoresed in 0.1% SDS, 4-12% gradient acrylamide gels. After electrophoresis, the gels were blotted on nitrocellulose membranes by semi-dry blotting (Bio-Rad Laboratories, Hercules, CA). The presence of immune complexes was identified by chemiluminescence ECL (Amersham Piscataway, NJ).

Cell proliferation and apoptosis assays

For proliferation assays, cells were cultured in 6 well tissue culture plates at 2.5×10^4 per well. Cell numbers were determined by trypsinization and counting in a hemocytometer. Alternatively, we used a colorimetric assay in the presence of 3-(4,5-dimethylthiazol carboxymethoxyphenyl)-2-(4-sulfophenyl)-2H tetrazolium salt (MTT; Promega, Madison, WI). For cell cycle analysis, cells were pulsed with BrdU for 40 min before being harvested and incubated in the presence of an FITC anti-BrdU mAb and 7-amino actinomycin D (7AAD) (BD Biosciences). For apoptosis assay, cells were cultured in 6 well plates (4.5×10^5 per well) for 48 h, washed with cold PBS twice and resuspended in Annexin V binding buffer. Annexin V and propidium iodide (PI) staining were performed according to the instructions of the manufacturer (Annexin V-FITC Apoptosis Detection Kit II, BD Biosciences). Caspase-3 activity was determined using the ApoTarget caspase-3/CPP32 colorimetric protease assay kit from Biosource International (Camarillo, CA) on aliquots containing 100 μg of proteins.

Flow Cytometry

Analyses were done using a FACSCAN flow cytometer and the data were analyzed using the Cell Quest software (BD Biosciences). SAOS-2 human osteosarcoma cells (positive for IL-6Rα/gp80 and gp130) and NIH3T3 (negative) cells were used as control.

Immunofluorescence

Cells were cultured in Lab-Tek II 8 chamber slides for 48 h at two different densities (2×10^4 and 1×10^5 cells/well). Cells were washed and fixed with 4% formaldehyde in PBS for 10 min and permeabilized with 0.1% Triton-X100, 15% FCS in PBS for 5 min, before being incubated with a goat anti-human IL-6 antibody (AF-206-NA, dilution 1:100, R& D Systems) overnight at 4°C followed by a mouse anti-human STRO-1 mAb for 3 h at 37°C. Dual immunofluorescence localization was achieved in the presence of a secondary Cy3 conjugated donkey anti-goat antibody and a FITC conjugated horse anti-mouse IgG antibody at 1:300 dilution for 45 min in darkness at room temperature. After washing with 0.1% Triton-X100 in PBS for 3 times, slides were mounted with DAPI containing Vectashield medium (Vector Laboratories, Burlingame, CA) and photographed under a Zeiss fluorescent microscope.

Analysis was also performed on paraffin embedded sections (4 μm) of bone marrow biopsies from 5 patients with neuroblastoma bone marrow metastasis. Sections were

deparaffinized in xylene, rehydrated, and treated with an antigen unmasking solution (citrate buffer pH 6.0, Vector Laboratories) for 10 min at 95°C. These sections were sequentially incubated in the presence of a goat anti-human IL-6 antibody and a mouse anti-human tyrosine hydroxylase mAb (dilution 1:1,000, Pel-Freez Arkansas, LLC). After washing, the slides were incubated in the presence of a FITC conjugated horse anti-mouse IgG antibody (dilution 1:2,000) and a Cy3 conjugated donkey anti-goat IgG (dilution 1:800). The slides were mounted in DAPI containing Vectashield medium.

Animal experiments

NOD/SCID mice were injected subcutaneously with 5×10^5 of CHLA-255/Luc mixed with 5×10^5 CHLA-225/IL-6 or 5×10^5 CHLA-255/control neuroblastoma cells in the left and right posterior thoracic side . After 4 weeks, mice were examined for bioluminescence as previously described (24). Animal experiments were performed according to a protocol approved by institutional Animal Care and Usage Committee of Childrens Hospital Los Angeles.

Statistical analysis

All assays were performed in triplicate. Comparisons between two groups were done by the unpaired Student's t-test and one way ANOVA using Tukey method of multiple comparisons. All reported p-values are two-sided.

Results

Neuroblastoma cells express IL-6R in the absence of IL-6 and sIL-6R

To explore whether IL-6 could have a paracrine or autocrine effect on neuroblastoma cells, we first examined the expression of IL-6Rα/gp80, gp130, IL-6 and sIL-6R in eleven human neuroblastoma cell lines by flow cytometry (IL-6Rα/gp80 and gp130) and ELISA (IL-6 and sIL-6R). The data (Table 1 and Supplemental data Fig. S1A) indicated the presence of the ubiquitous gp130 receptor protein in all cell lines and the presence of the IL-6Rα/gp80 protein in 9 cell lines. In contrast, IL-6 was detected in unconcentrated serum-free conditioned medium of only 4 cell lines and in 2 of these cell lines (CHLA-171 and SK-N-BE(2)) the levels were below 10 pg/ml. sIL-6R was not detected. Concentration of the conditioned medium to 10× did not result in the detection of IL-6 or sIL-6R in cell lines for which these proteins were undetected in unconcentrated serum-free medium (data not shown). These data were validated in 5 cell lines (CHLA-171, CHLA-255, SMS-SAN, SK-N-BE(2) and NB-19) by RT-PCR and Western blot analysis (Supplemental data Fig. S1*B* and *C*).

Neuroblastoma cells respond to exogenous IL-6

We then tested the response of these neuroblastoma cell lines to exogenous IL-6, by examining the effect of rhIL-6 on STAT-3 and Erk 1/2 activation, the 2 major signaling pathways downstream of IL-6. In CHLA-255 cells, we observed activation of STAT-3 and Erk 1/2 at concentrations of rhIL-6 ranging from 10 to 100 ng/ml with a maximum between 30 and 50 ng/ml of rhIL-6 (Fig. 1*A*). Activation of STAT-3 and Erk 1/2 occurred as early as 5 min after exposure to rhIL-6 and was maximal at 30 min (Fig. 1*B*). A similar activation of STAT-3 and Erk 1/2 was observed with CHLA-171, SMS-SAN, SK-N-BE(2) but not with NB-19 cells that did not express IL-6Rα/gp80 (Supplemental data Fig. S2*A* and *B*). Activation of STAT-3 but not Erk 1/2 was enhanced by the addition of sIL-6R (250 ng/ml), whereas activation of both signaling pathways was inhibited by a blocking antibody against IL-6Rα/gp80. STAT-3 activation was abrogated in the presence of AG490 (50 μM), and Erk 1/2 activation was blocked by PD98059 (100 μM) (Fig. 1*C* and *D*). Altogether the data

indicate that treatment of neuroblastoma cells that express IL-6Rα/gp80 and gp130 with rhIL-6 stimulates signaling pathways known to be downstream of its receptor, which suggest the presence of a functional receptor.

IL-6 produced by BMSC stimulates the proliferation of IL-6R positive but not IL-6R negative neuroblastoma cells

Because we had previously shown that human neuroblastoma cells stimulate the expression of IL-6 by BMSC in co-cultures (16), we initially explored whether BMSC would affect the proliferation of neuroblastoma cells in an IL-6-dependent manner. For these experiments, we selected CHLA-255 (IL-6R positive) and NB-19 (IL-6R negative) cells. We observed that CHLA-255 cells co-cultured in a transwell chamber in the presence of BMSC proliferated at a faster rate than when cultured alone (Fig. 2*A*). Consistent with our previous report (16), we detected a progressive increase in IL-6 production in the supernatant of the co-cultures (Supplemental data Fig. S3*A*). Confirming that the growth stimulatory effect of BMSC was mediated by IL-6, we found an absence of growth stimulation in the presence of a blocking antibody against IL-6Rα/gp80 (Fig. 2*A*). In contrast, co-culturing IL-6Rα/gp80 deficient NB-19 cells with BMSC had no effect on their rate of proliferation. We then documented that rhIL-6 (10 ng/ml) stimulated the growth of CHLA-255 cells both in the presence (Fig. 2*B*) or absence of serum (Supplemental data Fig. S3*B*). The growth stimulatory effect of rhIL-6 was dose dependent at concentrations ranging between 1 and 10^4 pg/ml and was neutralized in the presence of a blocking mAb against IL-6Rα/gp80 (Fig. 2*C*) that inhibited STAT-3 and Erk 1/2 activation (Supplemental data Fig. S3*D*). In contrast, and as anticipated, rhIL-6 had no growth stimulatory effect on NB-19 cells (Fig. 2*C*). To confirm that IL-6 stimulated cell proliferation, we examined its effect on cell cycle and BrdU incorporation. These experiments revealed an increased percent of BrdU positive cells in the presence of 10 ng/ml of IL-6 without an increase in apoptotic (BrdU negative, 7AAD positive) cells (Supplemental data Fig. S3*C*). This growth stimulatory effect appeared dependent on Erk 1/2 activation since it was inhibited in the presence of PD98059 (Supplemental data Fig. S3*D*) that blocked Erk 1/2 phosphorylation. However we could not rule out the possibility that STAT-3 activation provided an alternate signaling pathway because this inhibitor, which blocked the proliferative effect on CHLA-255, inhibited both Erk 1/2 and STAT-3 phosphorylation. We finally tested whether IL-6 could also have an autocrine growth stimulatory activity on neuroblastoma cells that express both the receptor and the cytokine. For this experiment, we tested the effect of a blocking anti-IL-6Rα/gp80 antibody on the proliferation of SK-N-RA cells that express IL-6R and IL-6 (Table 1). The data indicated a significant inhibition of proliferation in the presence of the blocking antibody when compared to cells incubated in the presence a non-specific mouse IgG (Supplemental data Fig. S3*E*). Altogether these data pointed to IL-6 having a growth stimulatory effect on neuroblastoma cells *in vitro*.

Paracrine IL-6 stimulates the growth of CHLA-255 neuroblastoma cells *in vivo*

We then tested whether IL-6 could also stimulate the proliferation of IL-6R positive neuroblastoma cells *in vivo*. For these experiments, we co-injected subcutaneously in NOD/SCID mice CHLA-255/Luc cells with CHLA-255 cells expressing IL-6 as a paracrine source of hIL-6 and used luciferin-induced bioluminescence to determine the effect of paracrine hIL-6 (made by CHLA-255/IL-6 cells) on the proliferation of CHLA-255/Luc cells. The data indicated a 5 fold increase in the average luminescence intensity when CHLA-255/Luc cells were co-injected with CHLA-255/IL-6 when compared to co-injection with CHLA-255/vector control cells (Fig. 2D). The data point to IL-6 having a growth-stimulatory activity on human neuroblastoma cells *in vivo* as *in vitro*.

IL-6 protects neuroblastoma cells from drug-induced apoptosis

It has been previously reported that the bone marrow microenvironment is a known sanctuary for tumor cells and protects them from the cytotoxic effect of chemotherapeutic agents (5). We therefore asked the question whether IL-6 could contribute to this effect by protecting neuroblastoma cells from drug-induced cytotoxicity. For these experiments we selected etoposide (VP-16), a podophylotoxin derivative and topoisomerase inhibitor used in the conventional treatment of patients with advanced neuroblastoma (26). We first demonstrated that etoposide induced apoptosis and increased caspase-3 activity in CHLA-255 cells in a dose-dependent manner (Fig. 3*A*). Selecting a concentration of etoposide of 0.25 μg/ml, we then examined whether the apoptotic effect of etoposide on neuroblastoma cells would be altered by the presence of BMSC. For this experiment, we compared CHLA-255 (IL-6R positive) and NB-19 (IL-6R negative) cells. The data (Fig. 3*B*) revealed a trend to a decrease in etoposide-induced apoptosis when CHLA-255 cells were co-cultured with BMSC that however was not statistically significant but was eliminated upon addition of an anti-IL-6Rα/gp80 blocking antibody. There was no similar trend with NB-19 cells. Co-culturing CHLA-255 cells with BMSC also inhibited the levels of caspase-3 activity in CHLA-255 cells exposed to etoposide (Supplemental data Fig. S4*A*). Considering that etoposide also induced apoptosis in BMSC and therefore may have decrease the production of IL-6 by these cells, the data suggested that IL-6 could have a protective effect on etoposide-induced apoptosis. To confirm this possibility, we examined the effect of rhIL-6 on etoposide-induced apoptosis in CHLA-255 and NB-19 cells. The data demonstrated that exposure of CHLA-255 to rhIL-6 prior to treatment with etoposide significantly inhibited apoptosis, whereas it had no significant effect on NB-19 cells (Fig. 3*C* and Supplemental data Fig. S4*B*). The data thus indicate that through the production of IL-6, BMSC protect IL-6R positive neuroblastoma cells from the cytotoxic effect of etoposide.

Cyclooxygenase-2 (Cox-2) induced by IL-6 in neuroblastoma cells provides an amplification loop for IL-6 expression

Because we had previously reported that the stimulation of IL-6 expression in BMSC by neuroblastoma cells is adhesion independent, we looked for the presence of a soluble factor in the medium of neuroblastoma cells that stimulates IL-6 expression. IL-6 has been shown to stimulate Cox-2 expression, and concomitantly prostaglandin E2 (PGE2), a secreted product of Cox-2 activity. PGE2 is also known to stimulate IL-6 expression (27). Therefore we tested whether IL-6 would affect Cox-2 expression in neuroblastoma cells. This experiment indicated an absence of expression of Cox-2 in neuroblastoma cells under basal conditions, but an induction of expression in the presence of rhIL-6 (10 ng/ml) that was abrogated in the presence of an anti-IL-6Rα/gp80 blocking antibody (Fig. 4*A*). Induction of Cox-2 expression by IL-6 was concomitantly associated with an increase in the amount of PGE2 secreted in the culture medium (Fig. 4*B*). We then demonstrated that treatment of BMSC with PGE2 increased the expression of IL-6 in a dose dependent manner (Fig. 4*C*). The data are consistent with the hypothesis that the induction of Cox-2 by IL-6 in neuroblastoma cells contributes to an amplification loop where IL-6-stimulated neuroblastoma cells secrete PGE2, further increasing IL-6 production by BMSC. To confirm this possibility, we tested whether blocking PGE2 production in IL-6-treated neuroblastoma cells by Celecoxib would suppress their capacity to induce expression in BMSC. The data (Fig. 4*D*) indicated a dose-dependent inhibition of PGE-2 in the supernatant of Celecoxib-treated CHLA-255 cells and a loss of IL-6 mRNA expression in BMSC incubated in the presence of the supernatant of Celecoxib-treated CHLA-255 cells. Celecoxib also inhibited the amount of IL-6 present in the supernatant of the co-cultures.

IL-6 is produced by BMSC-derived from patients with metastatic bone marrow disease and is increased in the serum and bone marrow of patients with neuroblastoma bone metastasis

The data reported so far were generated with established neuroblastoma cells line cultured *in vitro*. We considered that it was important to obtain evidence that IL-6 also contributed to neuroblastoma progression in patients. To accomplish this, we first examined the expression of IL-6 in bone marrow biopsies obtained from 5 patients with neuroblastoma bone metastasis by dual immunofluorescence to confirm the stromal origin of IL-6. The data (Fig. 5*A*) indicated that IL-6 was expressed in tyrosine hydroxylase negative stromal cells located around tyrosine hydroxylase positive tumor cells. However, it was not possible to demonstrate that these cells represent mesenchymal stem cells. We therefore decided to isolate BMSC from the bone marrow of 2 patients with metastatic disease. After isolation and passage in culture, we obtained adherent cells that expressed several mesenchymal markers like STRO-1 (76.2%), CD105 (89.4%), CD166 (99.9%), and CD44 (99.4%) as determined by FACS analysis. These cells also expressed IL-6 as documented by dual-immunofluorescence (Supplemental data Fig. S4*C*). IL-6 was detected in the culture medium of these cells after several passages in culture and its concentration was increased by 2 to 3 fold in the presence of 50× concentrated culture medium from CHLA-255 cells (Fig. 5*B*). These data provide evidence that BMSC are a source of IL-6 in the bone marrow of patients with neuroblastoma. Additional evidence that induction of IL-6 in the bone marrow microenvironment is an important mediator of neuroblastoma progression and bone metastasis was obtained by measuring the levels of IL-6 in 16 patients with neuroblastoma bone metastasis (Fig. 5*C*). Whereas we did not detect IL-6 in the serum and bone marrow supernatant of normal individuals, the mean levels of IL-6 were 97.9 pg/ml in the bone marrow supernatant (n=8) and 14.6 pg/ml in the serum (n=16) of these patients. Altogether these data providing evidence that IL-6 is increased in patients with metastatic neuroblastoma support our *in vitro* observations and are consistent with the concept that stromal-derived IL-6 in the bone marrow contribute to a microenvironment that promotes the proliferation and survival of neuroblastoma cells.

Discussion

In this paper we demonstrate that IL-6 expressed by BMSC has a paracrine effect on neuroblastoma cells, stimulating their proliferation and protecting them from drug-induced apoptosis. We also provide evidence for the presence of a Cox-2-dependent amplification loop that enhances the expression of IL-6 by BMSC in the presence of neuroblastoma cells. Finally, supporting a role for IL-6 in patients with neuroblastoma bone metastasis, we document that BMSC isolated from patients with neuroblastoma bone marrow metastasis express IL-6 and that patients with neuroblastoma bone metastasis have elevated levels of IL-6 in their serum and bone marrow.

It has been well recognized, in particular in multiple myeloma, that the interaction between stromal cells and tumor cells in the bone marrow contributes to tumor progression (6). For example, adhesion of myeloma cells to bone marrow stromal cells through members of the cell adhesion molecules family of proteins or integrins induces the expression of IL-6 by BMSC (28). Our data demonstrate a similar contribution of BMSC and IL-6 to the progression of neuroblastoma in the bone marrow, but point to an important difference. Whereas in myeloma, the induction of IL-6 by BMSC requires cell-cell contact, in neuroblastoma contact between tumor cells and BMSC is not required. Our data indicate that the release of PGE2 by IL-6-stimulated neuroblastoma cells is one of the soluble factors that contribute to the production of IL-6 by BMSC by contributing to an amplification loop. However other soluble factors can contribute, and we have recently shown that Galectin 3-

binding protein, a glycosylated protein produced by neuroblastoma cells that binds to Galectin-3, a receptor present on BMSC, also stimulates IL-6 expression by BMSC (29).

The effect of IL-6 on neuroblastoma cell proliferation has been the subject of previously conflicting reports. A growth promoting activity of IL-6 and sIL-6R in human and murine neuroblastoma cells was initially reported (30,31), whereas other investigators reported that MYCN overexpression down-regulates IL-6 in the SH-EP007 neuroblastoma cell line. They also demonstrated that IL-6 does not inhibit neuroblastoma cell proliferation but inhibits endothelial cell proliferation via the STAT-3 pathway and VEGF-induced neovascularization in the rabbit cornea assay (32). Our data, which demonstrate an increase in cell proliferation and an increase in BrdU incorporation in association with Erk 1/2 activation, are consistent with IL-6 having a growth stimulatory effect on neuroblastoma cells. The growth promoting activity of IL-6 was also demonstrated *in vivo* in mice co-injected with CHLA-255/Luc and CHLA-255/IL-6 cells. Whether IL-6 could inhibit endothelial cell proliferation and angiogenesis was however not explored. We also demonstrate that PD98059, which inhibits Erk 1/2 but not STAT-3 activation, prevents the growth stimulatory activity of IL-6. This suggests that the growth stimulatory effect of IL-6 on neuroblastoma cells is at least in part mediated through the Erk 1/2 pathway, as was previously reported in multiple myeloma (20). However since we also observed inhibition of growth stimulation by AG490, which inhibited both ERK 1/2 and STAT-3, we cannot rule out the possibility that STAT-3 provides an alternate pathway In B cells and renal cell carcinoma, IL-6 stimulates proliferation in a STAT-3 dependent manner (33,34). Our data indicate that in most cases, IL-6 has a paracrine effect on neuroblastoma cells (i.e., its source is not the tumor cells), but that in some cases, it can have an autocrine effect (i.e., its source is also in the tumor cells) as shown in SK-N-RA cells..

The protective effect of IL-6 on drug-induced apoptosis is reported here for the first time in neuroblastoma. Several IL-6-mediated signaling pathways have been implicated in chemoresistance (28,35,36). IL-6 induces survival by transcriptionally upregulating the x-linked inhibitor of apoptosis in cholangiocarcinoma cells (37). In multiple myeloma and colorectal cancer, STAT-3 activation upregulates the expression of survival proteins like survivin, cyclin D1, Bcl-XL, and Mcl-1 (38). The protective activity of IL-6 on drug-induced apoptosis may also involve regulation in the expression of multidrug resistance transporters (39). The mechanism by which IL-6 protects neuroblastoma cells from drug-induced apoptosis is not known at this point, but is currently actively investigated in our laboratory.

Supporting a role for stromal-derived IL-6 in patients with neuroblastoma bone metastasis, we demonstrated in bone marrow biopsies that IL-6 is expressed by cells in the bone marrow stroma and not by tumor cells. We also show that BMSC isolated and cultured from the bone marrow of 2 patients with metastatic disease express IL-6 and that the expression is enhanced in the presence of supernatant from neuroblastoma cells. The data thus support the concept that BMSC are an important source of IL-6 in the bone marrow, but do not exclude the possibility that other non-malignant cells also contribute. Further evidence supporting a role of IL-6 in bone metastasis in neuroblastoma was obtained by finding elevated levels of IL-6 in the serum and the bone marrow of patients with neuroblastoma bone metastasis. Elevated levels of IL-6 in the serum of patients with other cancers, such as myeloma, melanoma, Hodgkin's lymphoma, prostate and colon carcinoma, have been reported to correlate with a more severe outcome (40-43). Whether IL-6 levels in patients with neuroblastoma are indicators of poor clinical outcome will require a larger study. Altogether the data indicate that stromal-derived IL-6 in patients with neuroblastoma marrow metastasis, is an important contributor to tumor progression.

The data raise the possibility that IL-6 could be a valuable therapeutic target in patients with high-risk neuroblastoma. Several agents targeting IL-6 have been developed and some are currently tested in clinical trials in inflammatory diseases and malignancies. Tocilizumab, a humanized antibody against IL-6R (44), has been successfully used in patients with rheumatoid arthritis (45) and in children with systemic onset of juvenile rheumatoid arthritis (46). It is approved for the treatment of Castleman's disease, a lymphoproliferative disease associated with elevated levels of IL-6. More recently, a genetically engineered form of this antibody suitable for delivery by gene therapy has been shown to be effective in an IL-6-dependent multiple myeloma cell line *in vivo* (47). mAb against IL-6 is also currently being tested in clinical trials in myeloma in combination with melphalan and dexamethasone (48). Targeting IL-6 mediated Jak2/STAT-3 with small molecules, such as Capsacin and SD1008, is another approach currently tested in preclinical models of multiple myeloma (49) and ovarian cancer (50). Our data support the testing of IL-6 targeted therapies in clinical trials in children with advanced neuroblastoma.

Supplementary Material

Refer to Web version on PubMed Central for supplementary material.

Acknowledgments

Grant support: NIH/National Cancer Institute grant CA81403 (H. Shimada, R. Seeger, Y.A. DeClerck) and CA116548 (L. Metelitsa), Children's Neuroblastoma Cancer Foundation (T. Ara). We thank Ms. J. Rosenberg for her excellent assistance in preparing the manuscript, Dr. Laurence Blavier for her assistance in the experiments and Dr.Patrick Reynolds (Childrens Hospital Los Angeles) for providing several of the cell lines used in this study.

References

1. Liotta LA, Kohn EC. The microenvironment of the tumour-host interface. Nature 2001;411:375–9. [PubMed: 11357145]
2. Roskelley CD, Bissell MJ. The dominance of the microenvironment in breast and ovarian cancer. Semin Cancer Biol 2002;12:97–104. [PubMed: 12027581]
3. Bhowmick NA, Neilson EG, Moses HL. Stromal fibroblasts in cancer initiation and progression. Nature 2004;432:332–7. [PubMed: 15549095]
4. Fidler IJ. The pathogenesis of cancer metastasis: the ‘seed and soil’ hypothesis revisited. Nat Rev Cancer 2003;3:453–8. [PubMed: 12778135]
5. Hazlehurst LA, Landowski TH, Dalton WS. Role of the tumor microenvironment in mediating de novo resistance to drugs and physiological mediators of cell death. Oncogene 2003;22:7396–402. [PubMed: 14576847]
6. Mitsiades CS, Mitsiades NS, Munshi NC, Richardson PG, Anderson KC. The role of the bone microenvironment in the pathophysiology and therapeutic management of multiple myeloma: interplay of growth factors, their receptors and stromal interactions. Eur J Cancer 2006;42:1564–73. [PubMed: 16765041]
7. Kaplan RN, Rafii S, Lyden D. Preparing the “soil”: the premetastatic niche. Cancer Res 2006;66:11089–93. [PubMed: 17145848]
8. Dennis JE, Carbillet JP, Caplan AI, Charbord P. The STRO-1+ marrow cell population is multipotential. Cells Tissues Organs 2002;170:73–82. [PubMed: 11731697]
9. Prockop DJ. Marrow stromal cells as stem cells for nonhematopoietic tissues. Science 1997;276:71–4. [PubMed: 9082988]
10. Stewart K, Monk P, Walsh S, Jefferiss CM, Letchford J, Beresford JN. STRO-1, HOP-26 (CD63), CD49a and SB-10 (CD166) as markers of primitive human marrow stromal cells and their more differentiated progeny: a comparative investigation in vitro. Cell Tissue Res 2003;313:281–90. [PubMed: 12883998]

11. Jones EA, Kinsey SE, English A, et al. Isolation and characterization of bone marrow multipotential mesenchymal progenitor cells. Arthritis Rheum 2002;46:3349–60. [PubMed: 12483742]
12. Brodeur GM. Neuroblastoma: biological insights into a clinical enigma. Nat Rev Cancer 2003;3:203–16. [PubMed: 12612655]
13. Matthay KK, Villablanca JG, Seeger RC, et al. Treatment of high-risk neuroblastoma with intensive chemotherapy, radiotherapy, autologous bone marrow transplantation, and 13-cis-retinoic acid. Children's Cancer Group. N Engl J Med 1999;341:1165–73.
14. Dubois SG, Kalika Y, Lukens JN, et al. Metastatic sites in stage IV and IVS neuroblastoma correlate with age, tumor biology, and survival. J Pediatr Hematol Oncol 1999;21:181–9. [PubMed: 10363850]
15. Ara T, DeClerck YA. Mechanisms of invasion and metastasis in human neuroblastoma. Cancer Metastasis Rev 2006;25:645–57. [PubMed: 17160711]
16. Sohara Y, Shimada H, Minkin C, Erdreich-Epstein A, Nolta JA, DeClerck YA. Bone marrow mesenchymal stem cells provide an alternate pathway of osteoclast activation and bone destruction by cancer cells. Cancer Res 2005;65:1129–35. [PubMed: 15734993]
17. Heinrich PC, Behrmann I, Haan S, Hermanns HM, Muller-Newen G, Schaper F. Principles of interleukin (IL)-6-type cytokine signalling and its regulation. Biochem J 2003;374:1–20. [PubMed: 12773095]
18. Yamasaki K, Taga T, Hirata Y, et al. Cloning and expression of the human interleukin-6 (BSF-2/IFN beta 2) receptor. Science 1988;241:825–8. [PubMed: 3136546]
19. Skiniotis G, Boulanger MJ, Garcia KC, Walz T. Signaling conformations of the tall cytokine receptor gp130 when in complex with IL-6 and IL-6 receptor. Nat Struct Mol Biol 2005;12:545–51. [PubMed: 15895091]
20. Giuliani N, Lunghi P, Morandi F, et al. Downmodulation of ERK protein kinase activity inhibits VEGF secretion by human myeloma cells and myeloma-induced angiogenesis. Leukemia 2004;18:628–35. [PubMed: 14737074]
21. Murray PJ. The JAK-STAT signaling pathway: input and output integration. J Immunol 2007;178:2623–9. [PubMed: 17312100]
22. Jones SA, Horiuchi S, Topley N, Yamamoto N, Fuller GM. The soluble interleukin 6 receptor: mechanisms of production and implications in disease. FASEB J 2001;15:43–58. [PubMed: 11149892]
23. Kallen KJ. The role of transsignalling via the agonistic soluble IL-6 receptor in human diseases. Biochim Biophys Acta 2002;1592:323–43. [PubMed: 12421676]
24. Mouchess ML, Sohara Y, Nelson MD Jr. DeClerck YA, Moats RA. Multimodal imaging analysis of tumor progression and bone resorption in a murine cancer model. J Comput Assist Tomogr 2006;30:525–34. [PubMed: 16778634]
25. Alhadlaq A, Mao JJ. Mesenchymal stem cells: isolation and therapeutics. Stem Cells Dev 2004;13:436–48. [PubMed: 15345137]
26. Simon T, Langler A, Harnischmacher U, et al. Topotecan, cyclophosphamide, and etoposide (TCE) in the treatment of high-risk neuroblastoma. Results of a phase-II trial. J Cancer Res Clin Oncol 2007;133:653–61. [PubMed: 17479288]
27. Liu XH, Kirschenbaum A, Yao S, Levine AC. Cross-talk between the interleukin-6 and prostaglandin E(2) signaling systems results in enhancement of osteoclastogenesis through effects on the osteoprotegerin/receptor activator of nuclear factor-{kappa}B (RANK) ligand/RANK system. Endocrinology 2005;146:1991–8. [PubMed: 15618359]
28. Damiano JS, Cress AE, Hazlehurst LA, Shtil AA, Dalton WS. Cell adhesion mediated drug resistance (CAM-DR): role of integrins and resistance to apoptosis in human myeloma cell lines. Blood 1999;93:1658–67. [PubMed: 10029595]
29. Fukaya Y, Shimada H, Wang LC, Zandi E, DeClerck YA. Identification of Gal-3 binding protein as a factor secreted by tumor cells that stimulates interleukin-6 expression in the bone marrow stroma. J Biol Chem. 2008
30. Candi E, Knight RA, Spinedi A, Guerrieri P, Melino G. A possible growth factor role of IL-6 in neuroectodermal tumours. J Neurooncol 1997;31:115–22. [PubMed: 9049837]

31. Knezevic-Cuca J, Stansberry KB, Johnston G, et al. Neurotrophic role of interleukin-6 and soluble interleukin-6 receptors in N1E-115 neuroblastoma cells. J Neuroimmunol 2000;102:8–16. [PubMed: 10626661]
32. Hatzi E, Murphy C, Zoephel A, et al. N-myc oncogene overexpression down-regulates IL-6; evidence that IL-6 inhibits angiogenesis and suppresses neuroblastoma tumor growth. Oncogene 2002;21:3552–61. [PubMed: 12032857]
33. Hirano T, Ishihara K, Hibi M. Roles of STAT3 in mediating the cell growth, differentiation and survival signals relayed through the IL-6 family of cytokine receptors. Oncogene 2000;19:2548–56. [PubMed: 10851053]
34. Horiguchi A, Oya M, Marumo K, Murai M. STAT3, but not ERKs, mediates the IL-6-induced proliferation of renal cancer cells, ACHN and 769P. Kidney Int 2002;61:926–38. [PubMed: 11849447]
35. Hardin J, MacLeod S, Grigorieva I, et al. Interleukin-6 prevents dexamethasone-induced myeloma cell death. Blood 1994;84:3063–70. [PubMed: 7949178]
36. Chauhan D, Kharbanda S, Ogata A, et al. Interleukin-6 inhibits Fas-induced apoptosis and stress-activated protein kinase activation in multiple myeloma cells. Blood 1997;89:227–34. [PubMed: 8978296]
37. Yamagiwa Y, Marienfeld C, Meng F, Holcik M, Patel T. Translational regulation of x-linked inhibitor of apoptosis protein by interleukin-6: a novel mechanism of tumor cell survival. Cancer Res 2004;64:1293–8. [PubMed: 14973058]
38. Lassmann S, Schuster I, Walch A, et al. STAT3 mRNA and protein expression in colorectal cancer: effects on STAT3-inducible targets linked to cell survival and proliferation. J Clin Pathol 2007;60:173–9. [PubMed: 17264243]
39. Lee G, Piquette-Miller M. Cytokines alter the expression and activity of the multidrug resistance transporters in human hepatoma cell lines; analysis using RT-PCR and cDNA microarrays. J Pharm Sci 2003;92:2152–63. [PubMed: 14603501]
40. Tas F, Oguz H, Argon A, et al. The value of serum levels of IL-6, TNF-alpha, and erythropoietin in metastatic malignant melanoma: serum IL-6 level is a valuable prognostic factor at least as serum LDH in advanced melanoma. Med Oncol 2005;22:241–6. [PubMed: 16110135]
41. Pedersen LM, Klausen TW, Davidsen UH, Johnsen HE. Early changes in serum IL-6 and VEGF levels predict clinical outcome following first-line therapy in aggressive nonHodgkin's lymphoma. Ann Hematol 2005;84:510–6. [PubMed: 15834569]
42. George DJ, Halabi S, Shepard TF, et al. The prognostic significance of plasma interleukin-6 levels in patients with metastatic hormone-refractory prostate cancer: results from cancer and leukemia group B 9480. Clin Cancer Res 2005;11:1815–20. [PubMed: 15756004]
43. Belluco C, Nitti D, Frantz M, et al. Interleukin-6 blood level is associated with circulating carcinoembryonic antigen and prognosis in patients with colorectal cancer. Ann Surg Oncol 2000;7:133–8. [PubMed: 10761792]
44. Nishimoto N, Kishimoto T. Interleukin 6: from bench to bedside. Nat Clin Pract Rheumatol 2006;2:619–26. [PubMed: 17075601]
45. Paul-Pletzer K. Tocilizumab: blockade of interleukin-6 signaling pathway as a therapeutic strategy for inflammatory disorders. Drugs Today (Barc) 2006;42:559–76. [PubMed: 17028666]
46. Yokota S, Miyamae T, Imagawa T, Katakura S, Kurosawa R, Mori M. Clinical study of tocilizumab in children with systemic-onset juvenile idiopathic arthritis. Clin Rev Allergy Immunol 2005;28:231–8. [PubMed: 16129907]
47. Yoshio-Hoshino N, Adachi Y, Aoki C, Pereboev A, Curiel DT, Nishimoto N. Establishment of a new interleukin-6 (IL-6) receptor inhibitor applicable to the gene therapy for IL-6-dependent tumor. Cancer Res 2007;67:871–5. [PubMed: 17283116]
48. Rossi JF, Fegueux N, Lu ZY, et al. Optimizing the use of anti-interleukin-6 monoclonal antibody with dexamethasone and 140 mg/m2 of melphalan in multiple myeloma: results of a pilot study including biological aspects. Bone Marrow Transplant 2005;36:771–9. [PubMed: 16113665]
49. Bhutani M, Pathak AK, Nair AS, et al. Capsaicin is a novel blocker of constitutive and interleukin-6-inducible STAT3 activation. Clin Cancer Res 2007;13:3024–32. [PubMed: 17505005]

50. Duan Z, Bradner J, Greenberg E, et al. 8-benzyl-4-oxo-8-azabicyclo[3.2.1]oct-2-ene-6,7-dicarboxylic acid (SD-1008), a novel janus kinase 2 inhibitor, increases chemotherapy sensitivity in human ovarian cancer cells. Mol Pharmacol 2007;72:1137–45. [PubMed: 17675586]

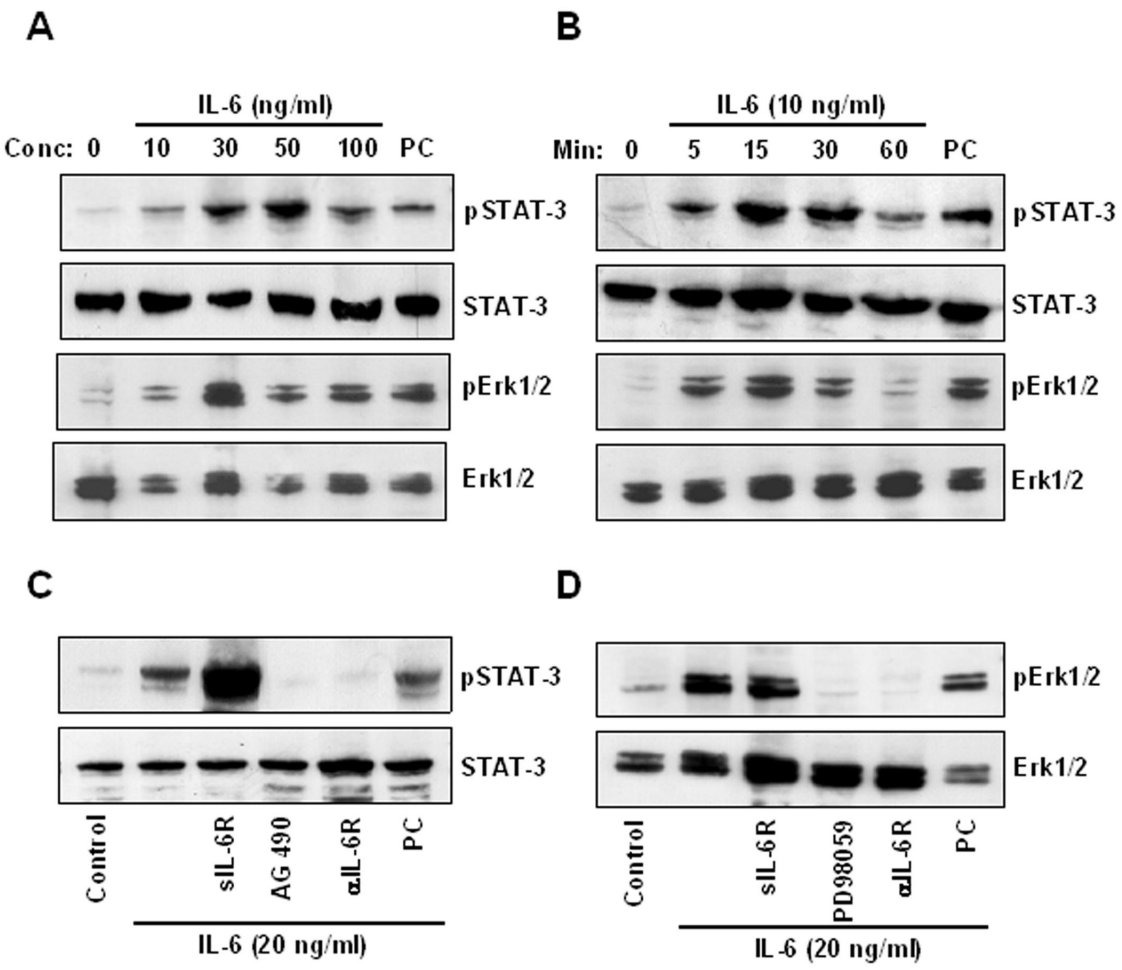

Figure 1.

IL-6 activates STAT-3 and Erk 1/2 in IL-6R positive CHLA-255 neuroblastoma cells. *A*, expression of phospho-STAT-3 (pSTAT-3), STAT-3, phospho-Erk 1/2 (pErk 1/2) and Erk 1/2 examined by Western blot analysis in total cell lysates (20 μg) of CHLA-255 cells collected 15 min after treatment with rhIL-6 at indicated concentrations. As positive control (PC) we used lysates from interferon-γ treated HELA cells (Cell Signaling Technology, Beverly, MA). *B*, cell lysates (20 μg) of CHLA-255 cells treated with rhIL-6 (10 ng/ml) for indicated time were collected and examined for pSTAT-3, STAT-3, pErk 1/2 and Erk 1/2 by Western blot. *C*, CHLA-255 cells were treated with sIL-6R (250 ng/ml), AG490 (50 μM) or an anti IL-6R antibody (2 μg/ml) prior to being exposed to rhIL-6 (20 ng/ml) for 15 min. Cell lysates were then examined for pSTAT-3 and STAT-3 expression by Western blot as in *(A)* and *(B)*. IL-6 treated SAOS-2 cells were used as PC. *D*, same experiment as in *(C)*, but cells were treated with PD98059 (100 μM) in lieu of AG490 and examined for the expression of pErk 1/2 and Erk 1/2. The data in *(A)* to *(D)* are representative of one experiment from 3 separate experiments showing similar results.

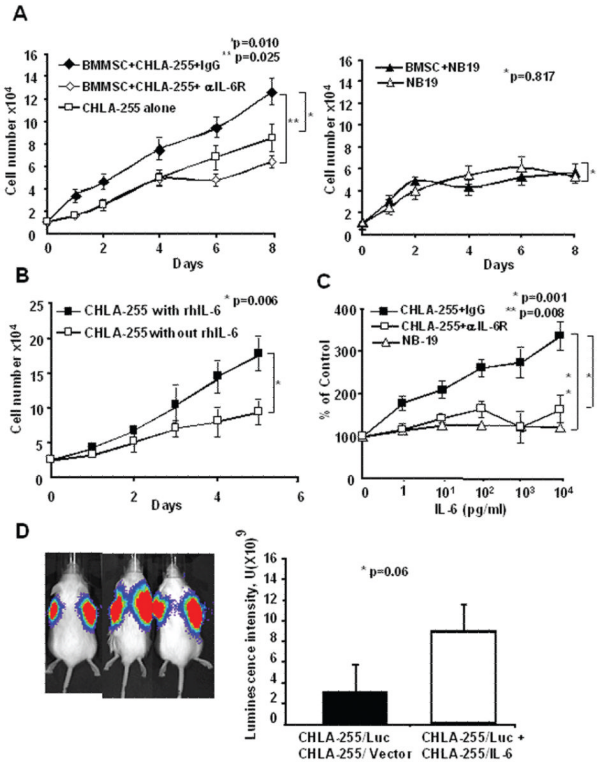

Figure 2.

BMSC stimulate neuroblastoma cell proliferation in an IL-6-dependent manner. *A*, BMSC (2.5×10^4 cells/well) and CHLA-255 cells (left panel) or NB-19 cells (right panel) (1×10^5 cells/well) were co-cultured in transwell tissue culture plates. The culture medium was changed on day 4 and when indicated an anti IL-6R antibody (2 μg/ml) was added on day 0 and day 4. Cells were counted after trypsinization. The data represent the average numbers of cells per well (±SD) of triplicate samples. *B*, CHLA-255 cells were cultured in the presence of serum with or without rhIL-6 (10 ng/ml) added on day 0, 2 and 4. Cells were counted at the indicated times. The data represent the average cell numbers (±SD) per dish of triplicate dishes. *C*, CHLA-255 and NB-19 cells were cultured for 4 days with rhIL-6 at indicated concentrations. An anti IL-6R antibody (2 μg/ml) or control mouse IgG (0.2 μg/ml) was added to the culture medium of CHLA-255 cells on day 0 and 2. The number of viable cells was determined using an MTT assay as described in Materials and Methods. The data represent the mean percent (±SD) of the control (no IL-6) at day 4 from triplicate samples. *D*. NOD/SCID mice were subcutaneously co-injected in the right side with CHLA-255/Luc cells and CHLA-255/IL-6 cells and in the left side with CHLA-255/Luc and CHLA-255/vector (control) cells. Left panel: representative bioluminescence data on 3 mice obtained 4 weeks after tumor cell injection. Right panel: mean luminescence intensity (±SD) of the data obtained from 7 mice. The data are representative of 2 separate experiments showing similar results.

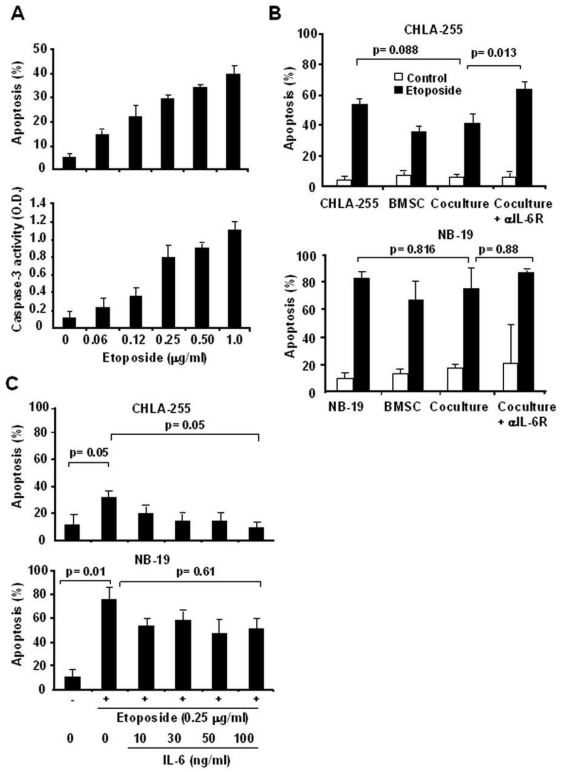

Figure 3.

BMSC protect neuroblastoma cells from etoposide-induced apoptosis in an IL-6 dependent manner. *A*, CHLA-255 cells were exposed to etoposide at indicated concentrations for 24 h and examined for apoptosis by Annexin-V staining (top panel) and caspase-3 activity (lower panel) as described in Materials and Methods. The data represent the mean values (±SD) of 3 separate samples. *B*, BMSC (2.5×10^4 cells/well) and CHLA-255 (top panel) or NB-19 (bottom panel) (1×10^5 cells/well) cells were cultured alone or together in transwell tissue culture plates for 48 h in the presence or absence (control) of etoposide (0.25 μg/ml added after 24 h of culture). The cells were then examined for apoptosis. An antibody against IL-6R (2 μg/ml) was added as indicated. The data represent the mean (±SD) values of triplicate samples and are representative of 3 experiments showing similar results. *C*, CHLA-255 and NB-19 cells were incubated with rhIL-6 at indicated concentrations for 2 h before being exposed to etoposide. After 14 h, cells were examined for apoptosis. The data represent the mean (±SD) values of triplicate samples.

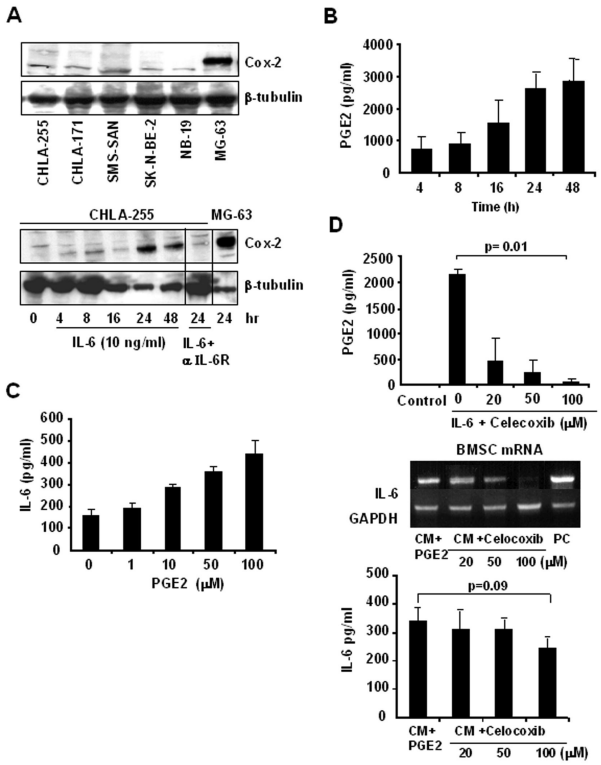

Figure 4.

IL-6 induces Cox-2 expression in neuroblastoma cells. *A*, *top*: Western blot analysis of Cox-2 expression in 5 neuroblastoma cell lines and MG-63 osteosarcoma cells (used as positive control); *bottom*: CHLA-255 cells were treated with rhIL-6 and examined at indicated times for Cox-2 expression by Western blot analysis. An antibody against IL-6R (2 μg/ml) was added 2 h before IL-6 when indicated. The data are representative of one experiment from 3 separate experiments showing similar results. *B*, PGE2 levels were measured by ELISA in the supernatant of CHLA-255 cells treated with IL-6 as shown in panel A, *bottom*. The data represent the mean (±SD) values of triplicate samples. *C*, BMSC were treated with PGE2 at indicated concentrations for 24 h and examined for IL-6 production in the culture medium by ELISA. The data represent the mean IL-6 (±SD) values of triplicate samples. *D*, CHLA-255 cells were treated with rhIL-6 (10 ng/ml) for 24 h in the absence or presence of Celecoxib at indicated concentrations. The supernatants were then collected and an aliquot examined for the presence of PGE2 (upper panel). The supernatants were then added to cultured BMSC for 24 h, before the cells were lysed and examined for IL-6 mRNA expression by RT-PCR and IL-6 protein by ELISA. The data represent the mean (±SD) values of triplicate samples.

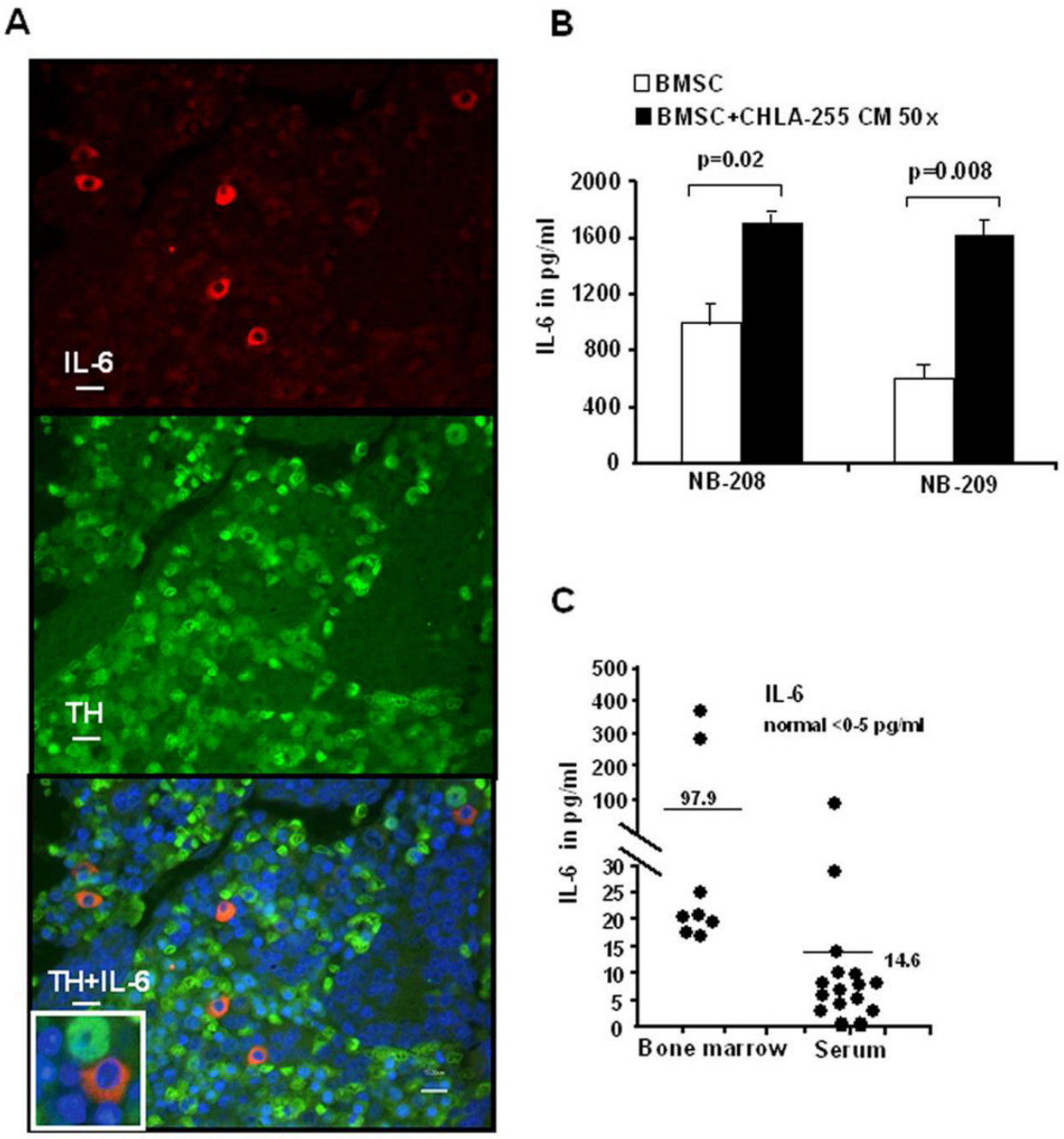

Figure 5.

Expression of IL-6 in BMSC derived from patients with metastatic neuroblastoma. *A*, Paraffin embedded histological sections of a bone marrow biopsy specimen from a patient with bone marrow neuroblastoma metastasis showing the expression of IL-6 in tyrosine hydroxylase (TH) negative stromal cells. *Top*: Cy3-anti IL-6; *middle:* FITC anti-TH; *bottom:* merge figure. Scale bar=10 μm. Inset in left upper panel is a 2 × enlargement of the area shown by the white . *B*, IL-6 levels in the medium of BMSC from patient NB-208 and NB-209 cultured for 24 h in the presence of regular medium or 50× concentrated conditioned medium from CHLA-255 cells were measured by ELISA. The data represent the mean (±SD) values of triplicate samples. *C*, IL-6 levels in the bone marrow (n=8) and

serum (n=16) of patients with neuroblastoma bone metastasis. The bars indicate the mean levels.

Table 1

Expression of IL-6Rα/gp180, gp130, IL-6 and sIL-6R in human neuroblastoma cell lines

NB cell line	MYCN status	gp130 % of cells	IL-6Rα/gp80 % of cells	IL-6 pg/ml	sIL-6R pg/ml
CHLA-42	N	49.83	73.07	0	0
CHLA-90	N	99.95	99.81	274	0
CHLA-119	N	68.10	97.81	0	0
CHLA-171	N	68.89	96.48	3.1	0
CHLA-255	N	99.41	97.80	0	0
LAN-6	N	96.48	91.20	0	0
NB-19	N	69.48	0.40	0	0
SH-5Y-SY	N	98.76	0.40	0	0
SK-N-BE(2)	A	82.64	92.62	6.6	0
SK-N-RA	N	85.00	98.67	236	0
SMS-SAN	A	97.46	95.38	0	0

The expression of gp130 and IL-6Ra/gp80 was determined by flow cytometry as shown in supplemental data figure S1A. Expression of IL-6 and sIL-6R was determined by ELISA and the data represent the mean concentrations in serum free medium after 24 h.